Physics – Uspekhi **53** (9) 915 – 921 (2010)

INSTRUMENTS AND METHODS OF INVESTIGATION PACS numbers: 95.55.Vj, 95.85.Ry, 96.50.S –

Ice satellites of planets of the Solar System and the on-orbit radio detection of ultrahigh-energy particles

G A Gusev, B N Lomonosov, V A Ryabov, V A Chechin

DOI: 10.3367/UFNe.0180.201009c.0957

Contents

Abstract. The problem of detecting nature's most energetic particles — cosmic rays and neutrinos — is reviewed. Prospects for using orbital radio detectors for these highest-energy particles are examined. Apertures are calculated for space experiments using the Moon and similar-sized ice satellites of planets of the Solar System as targets for the interaction of cosmic-ray particles and neutrinos. A comparative analysis shows that using the Moon as a target is the most promising scenario.

1. Introduction

Studies into the nature and spectra of cosmic particles having the highest energies in the Universe is one of the most topical issues of modern science [1–7]. Information on the nature of such particles is important for solving fundamental problems of astrophysics and particle physics related to sources and acceleration mechanisms of cosmic rays, as well as to the nature of dark matter [8].

The ability of present-day and future experiments to register ultrahigh-energy cosmic rays (UHECRs) is determined by the aperture of the detector in use. Despite the progress in the development of UHECR detectors there is an ambiguity in the interpretation of experimental data in which the restored energy of the primary particle exceeds $E_{\rm CR} \approx 10^{20}$ eV. First and foremost, this is due to insufficiently large apertures, even of giant ground-based detectors spread across an area of several thousand square kilometers.

The main goal of present-day neutrino astronomy is the detection of ultrahigh-energy neutrinos (UHENs). Such neutrinos can be produced in remote astrophysical sources from superheavy particle decays, as well as during the propagation of UHECRs in the interstellar medium. New-generation neutrino telescopes under construction have sensitivity volumes exceeding 1 km^3 and allow the detection of neutrinos with energies of up to $E_\nu \approx 10^{19}$ eV. However, if the neutrino flux turns out to be lower than that predicted by the most elaborated models, the exposed volumes of water and ice (~ 1 km^3) will be insufficient for its detection.

To detect cosmic rays and neutrinos with energies $E \geqslant 10^{20}$ eV, new detectors based on novel principles and using modern registration methods are required. In recent years, a method based on registration of coherent Cherenkov radio emission from cascades generated by ultrahigh-energy particles has become wide-spread. The most important advantage of the radio detection method includes the possibility of browsing through huge volumes that are transparent to radio emission and the registration with high statistical confidence of rare events at ultrahigh energies.

In the present paper, we consider the prospects of detection of UHECRs and UHENs by orbital radio detectors. The detection potential is determined from a comparison of apertures of space experiments which utilize the surface layer of the Moon and exotic ice satellites of Jupiter and Saturn [10] as targets for the interparticle interaction. It should be noted that the Luna-Glob space mission planned for launch in the near future includes the lunar orbital radio detector LORD (Lunar Orbital Radio Detector) [11–14]. Further into the future, missions to Jupiter's satellites are planned, so ice planets of Solar System are considered as likely targets for registration of UHECRs and UHENs by the radio detection method.

2. Problem of detection of ultrahigh-energy cosmic rays and neutrinos

The main difficulty in detecting UHECRs is related to their extreme rarity. If the integral UHECR flux amounts to ~ 1 km^{-2} yr^{-1} at energies $E_{\rm CR} \geqslant 10^{19}$ eV, at energies $E_{\rm CR} \geqslant 10^{20}$ eV the flux reduces to not more than one particle

G A Gusev, B N Lomonosov, V A Ryabov, V A Chechin
P N Lebedev Physical Institute, Russian Academy of Sciences,
Leninskii prosp. 53, 119991 Moscow, Russian Federation
Tel. (7-499) 135 42 95. E-mail: ryabov@x4u.lebedev.ru

Received 16 February 2010, revised 25 March 2010
Uspekhi Fizicheskikh Nauk **180** (9) 957 – 964 (2010)
DOI: 10.3367/UFNr.0180.201009c.0957
Translated by K A Postnov; edited by A Radzig

per 1 km^2 per century. In total, the Haverah Park [15], SUGAR (Sydney University Great Air Shower Ring) [16], Yakutsk [17], AGASA (Akeno Giant Air Shower Array) [18], Fly Eyes [19], and HiRes [20] experiments have registered only several dozen UHECR showers with energies $E_{CR} > 5 \times 10^{19}$ eV. Clearly, to detect UHECRs, vast-area detectors are needed, which register secondary particles of an extensive air shower (EAS). Currently, a new generation of UHECR detectors with huge apertures are operating, including the recently constructed P. Auger Observatory [21, 22] and Telescope Array [23]. The total area covered by the Auger and Telescope Array detectors reaches 3×10^3 km^2 and about 10^3 km^2, respectively. However, these detectors are apparently close to the area limit for ground-based detectors.

The employment of space detectors is the next step in registering particles with ultimately high energies. In the JEM–EUSO (Japanese Experiment Module – Extreme Universe Space Observatory) project, a detector will be installed on the International Space Station [24] to watch the fluorescent radiation created by UHECR air showers in the shadowed part of Earth's atmosphere. In addition, Cherenkov radiation reflected by the surface of the seas and oceans can be detected. The effective aperture of the JEM–EUSO detector will be about 10^5 km^2 sr. Somewhat smaller is the TUS (Track Setup) project in Russia, which will be realized in the nearest future [25]. Space-based experiments will also be capable of registering horizontal air showers initiated by high-energy neutrinos.

It could be quite possible that apertures of the Auger, Telescope Array, and even EUSO detectors would be insufficiently large to detect reliably UHECRs with energies $E_{CR} \geqslant 10^{20}$ eV (if they exist in the Universe).

It is natural to expect that a small fraction of the UHECR flux can be due to UHENs [6, 7]. To date, astrophysical neutrinos have been registered only from two low-energy sources — the Sun and supernova SN 1987A. However, there are serious grounds to believe that the astrophysical and cosmological sources of neutrinos with energies spanning more than 10 orders of magnitude — from about 10^{12} eV to $10^{22}-10^{24}$ eV — are also present. Possible astrophysical sources where protons and nuclei can be accelerated up to energies of $\sim 10^{20}$ eV include gamma-ray bursts [26–29] and active galactic nuclei [30–32]. In such space 'accelerators', pp- and pγ-interactions must produce charged pions decaying into UHENs with energies up to $E_\nu \approx 10^{19}$ eV [33–35]. Neutrino fluxes could also be generated in decays or annihilations of relic superheavy particles produced in the early Universe and surviving up to now [36]. Maximum neutrino energies in such scenarios depend on the mass of decaying heavy particles and can reach $E_\nu \approx 10^{24}$ eV [37–40]. The interaction of UHECRs with cosmic microwave background photons is the 'guaranteed' source of UHENs. Decays of pions produced in photoproduction reactions generate the so-called cosmogenic neutrino flux first calculated by Berezinsky and Zatsepin [41]. The energy spectrum of the cosmogenic flux has a maximum at energies $E_\nu \approx 10^{19}$ eV; however, the value of this flux is indefinite due to the unknown form of the initial proton spectrum in sources, the proton source distribution over redshifts, and their evolution [42–47]. The possibility of measuring the cosmogenic neutrino flux is usually considered as the starting point in optimizing apertures of the planned neutrino detectors. Neutrino fluxes calculated for different available models are shown in Fig. 1.

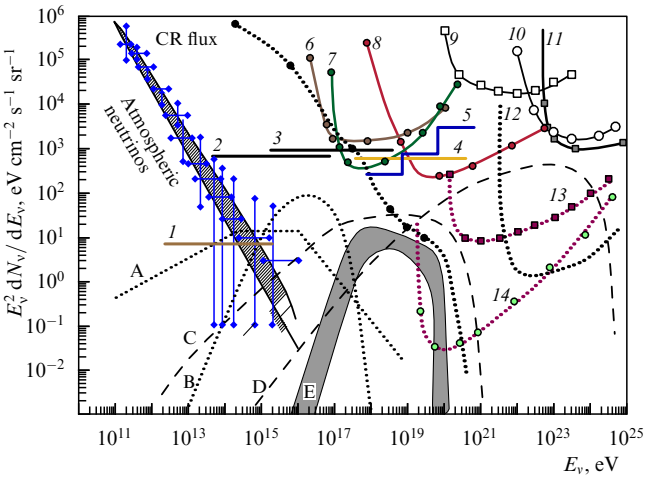

Figure 1. Experimental bounds on the diffuse neutrino flux at the 90% confidence level for the total neutrino composition homogeneous in flavors, viz. $\nu_e : \nu_\mu : \nu_\tau = 1:1:1$, assuming approximately the E_ν^{-2}-shaped energy spectrum (*1–11*). Horizontal lines show the integral limits of the neutrino flux derived from experiments: *1* — Ice Cube ($\nu_\mu \times 3$) [48], *2* — Baikal [49], *3* — AMANDA [50], *4* — RICE [51], and *5* — HiRes [the limit on the total flux $(\nu_e + \nu_\tau) \times 3/2$] [52]. Curves *6–11* correspond to differential limits: *6* — Ice Cube [48], *7* — Auger ($\nu_\tau \times 3$) [22], *8* — ANITA [53, 54], *9* — GLUE [55], *10* — FORTE [56], and *11* — Nu-Moon/WSRT [57, 58]. Curves *12* and *13* conform to calculated differential limits on the neutrino flux to be achieved in future experiments: *12* — LOFAR [59], and *13* — LORD. Curve *14* matches the calculated differential limit of the cosmic ray flux to be achieved in the LORD experiment. Curves A and B show calculated neutrino fluxes from various astrophysical sources: A — the main outburst in a gamma-ray burst [34], and B — active galactic nuclei [35]; C and D stand for 'top-down' scenarios [39] for heavy particle decays with masses $M_X = 2 \times 10^{21}$ eV and $M_X = 2 \times 10^{25}$ eV, respectively. The hatched region E corresponds to the uncertainties in the cosmogenic neutrino fluxes calculated in different approximations [45–47]. The atmospheric neutrino flux is shown for comparison with astrophysical fluxes: points show the $\nu_\mu + \bar{\nu}_\mu$ flux as measured by Ice Cube [60]; the hatched region restricts the model predictions [61–66]. The approximation of the cosmic ray flux is also illustrated [67].

To register UHENs with energies $E_\nu \geqslant 10^{19}$ eV, neutrino detectors with a volume of more than 1 km^3 are required [7]. Such detectors include natural volumes of pure water or ice, which can be simultaneously utilized as targets for neutrino interactions and radiators for generating Cherenkov radiation by secondary particles produced by virtue of neutrino reactions. At present, several neutrino telescopes are under construction in the Mediterranean Sea (ANTARES (Astronomy with a Neutrino Telescope and Abyss environmental RESearch) [68], NESTOR (Neutrino Extended Submarine Telescope with Oceanographic Research Project) [69], NEMO (NEutrino Mediterranean Observatory) [70], and KM3NeT (km3-size Neutrino Telescope) [71]), and in the Antarctica [AMANDA (Antarctic Muon And Neutrino Detector Array)/Ice Cube] [48, 50, 72] with the exposed volumes of water or ice of more than 1 km^3.

3. Radio detection of cosmic rays and neutrinos

To register particles with the highest energies, detectors working on new principles are needed. First of all, these are experiments which detect coherent radio emission from cascades initiated by neutrino interactions in radio-transparent natural media, such as the atmosphere [LOFAR (LOw Frequency ARray)] [59], the ice shields of Greenland

[FORTE (Fast on-Orbit rapid Recording of Transient Events)] [56] and Antarctica (RICE (Radio Ice Cherenkov Experiment) [51], ARIANNA (Antarctic Ross Ice shelf ANtenna Neutrino Array) [73], and ANITA (ANtarctic Impulsive Transient Antenna) [53, 54]), and salt minefields [SalSA (Salt dome Shower Array)] [74]. Some experiments use the radio-transparent near-surface layer of lunar soil (regolith) as a target to register UHECRs and UHENs; here, the radio emission from cascades is observed (or is planned to be observed) utilizing ground-based radio telescopes (Parkes [75], GLUE (Goldstone Lunar Ultra-high energy neutrino Experiment) [55], NuMoon [57], WSRT (Westerbork Synthesis Radio Telescope) [58], LUNASKA (Lunar Ultra-high energy Neutrino Astrophysics using the Square Kilometer Array) [76–78]) or radio receivers aboard circumlunar satellites (LORD [11–14]).

The radio method for detection of cosmic rays and neutrinos was first proposed by G A Askar'yan as early as the beginning of the 1960s [79, 80]. When a charged particle moves in a medium with a velocity v exceeding the phase speed of light in this medium ($v > c/n$, where n is the refraction coefficient of the medium), Vavilov–Cherenkov radiation is known to appear. In the optical range, this radiation is widely used to register both individual relativistic particles and particle cascades. As the pair creation processes and bremssrahlung radiation in the Coulomb field of atomic nuclei (which determine the cascade development at high energies of the shower particles) are charge-symmetrical, in the first approximation (with account of only high-energy shower particles) the shower is electrically neutral. When the radiation wavelength exceeds the distance between the particles in a shower, the destructive interference must lead to cancellation of emission from positively and negatively charged particles. Because of this, the shower is expected to not radiate in the radio frequency range. However, as was first noted by G A Askar'yan [79, 80], a significant number of the shower particles have energies of the order of 30 MeV and lower, at which the interaction not only with nuclei but also with atomic electrons becomes significant:

$$\gamma + e_{at}^- \to \gamma + e^-, \quad e^+ + e_{at}^- \to e^+ + e^-,$$
$$e^- + e_{at}^- \to e^- + e^-.$$

This interaction leads to a 'pulling out' of electrons from atoms of the surrounding medium into the shower, and the charge asymmetry of the shower emerges, i.e., an excess of negative charges in the shower disk. Calculations show that this excess adds up to 20–30% of the total number of shower electrons. Fast electrons from this excess with energies exceeding the Cherenkov radiation threshold emit radio waves.

The most important advantage of the radio detection method is the possibility of using a very long propagation length of radio waves, which allows watching huge volumes of the atmosphere and other radio-transparent media and detecting rare ultrahigh-energy events with high statistical significance. The application of the radio detection method is especially profitable at ultrahigh energies since the power of the coherent radio signal increases as the square of the shower energy, and at high energies the power of radio emission exceeds that in the optical range [9].

By the present time, the radio detection method of UHENs using ice targets has been tested in the FORTE [56], RICE [51], and ANITA [53, 54] experiments. In the FORTE experiment, the ice block of Greenland was browsed through from a low-orbit satellite. The satellite had two broadband log-periodic antennae which controlled the ice volume equal approximately to 1.8×10^6 km^3. The RICE experiment uses 20 dipole antennae with radio receivers frozen into the Antarctica ice at depths of 100–300 m. In the ANITA experiment, the radio wave detection is made by 36 horn antennae which scan an ice target of $\approx 9 \times 10^5$ km^3 during aerostat flights at an altitude of ~ 40 km above Antarctica. To date, two aerostat flights have been made with a total duration of 66 days. The analysis of radio signals detected in all these experiments has not revealed any candidates for UHEN interactions in the ice. The upper limits of the diffuse neutrino flux obtained in the FORTE, RICE, and ANITA experiments are given in Fig. 1.

It should be emphasized that experiments with ground ice targets (blocks in Greenland and Antarctica) can detect only cascades initiated by superhigh-energy neutrinos, since cosmic rays (protons and nuclei) do not reach the ice target and start interacting already in the upper layers of the terrestrial atmosphere.

4. Satellites of planets of the Solar System as targets for the detection of cosmic rays and neutrinos

The idea of employing the Moon as a target for detection of UHECRs and UHENs by the radio method was first proposed by G A Askar'yan [80]. In essence, the production of cascades and the generation of radio waves occur in the near-surface layer of the lunar soil, viz. the radio-transparent regolith, which consists of small particles and stones ejected by meteorite impacts with the Moon. The depth of the regolith is usually 10–30 m. Radio emission is generated by a cascade initiated by a high-energy particle within a solid angle close to the Cherenkov cone in a wide frequency band. Part of this emission after refraction at the 'regolith–vacuum' boundary comes out of the lunar soil and can be registered by a radio telescope. As the Moon has no atmosphere, both UHECR and UHEN interactions with the lunar soil can be detected.

In paper [81], R D Dagkesamanskii and I M Zheleznykh proposed using ground-based telescopes for the purpose. The Australia Parkes Observatory 64-m radio telescope was first used in 1996 to search for radio emission from lunar limb cascades for 2 hours [75]. In the GLUE experiment, two NASA's radio telescopes with mirror diameters of 70 m and 34 m, separated by a distance of 22 km, were used. The total time of observations of radio pulses generated by neutrino interactions in the lunar regolith was about 120 hours. The first measurements in the NuMoon experiment [57] were performed utilizing the WSRT telescope array consisting of fourteen 25-m parabolic antennas positioned along a 2.7-km line. Two separated beams were formed, each covering 1/3 of the lunar surface. The maximum registration time of cascades from ultrahigh-energy particles comprised 46.7 h [58]. Further measurements are planned by using the LOFAR antenna array located across the area of 3×10^4 km^2 [59]. The LOFAR phased-array radio telescope can be used to detect UHECRs and UHENs by radio emission from cascades generated both in Earth's atmosphere and the lunar regolith. The upper limits of the neutrino flux from the GLUE and NuMoon/WSRT experiments, as well as the calculated LOFAR limit, are presented in Fig. 1.

Paper [11] for the first time proposed detecting radio emission from UHECRs and UHENs using a circumlunar satellite in the LORD experiment. Limits on the UHECR and UHEN fluxes that can be obtained in one-year observations in the LORD experiment in the near-lunar orbit are also shown in Fig. 1. These limits are significantly higher than those in the most ambitious Auger and ANITA projects currently under way. Such a high registration potential of UHECRs and UHENs is due to the large apertures of the LORD radio detector. For cosmic rays with energies $E_{\rm CR} \geqslant 10^{20}$ eV, the total LORD aperture measures 2×10^5 km^2 sr, which is almost two orders of magnitude larger than that of the Auger observatory.

To estimate the prospects of radio detection of UHECRs and UHENs, we studied the possibility of using as targets the moons of Jupiter [Ganymede (radius $R_0 = 2631$ km) and Europa ($R_0 = 1561$ km)], and of Saturn [Rhea ($R_0 = 764$ km), Tethys ($R_0 = 528$ km), Dione ($R_0 = 559$ km), and Enceladus ($R_0 = 252$ km)]. These moons are unique objects in the Solar System since they almost entirely consist of ice, with a small addition of rocks in the internal layers [10].

In the first approximation, the moons Ganymede, Europa, Rhea, Tethys, Dione, and Enceladus can be considered as ice spherical targets of different radii.

5. Calculation of the registration aperture of cosmic rays and neutrinos in space experiments

Figure 2 illustrates the scheme of registration of radio emission from UHECRs and UHENs by a radio detector from an orbital spacecraft.

An incident particle interacts with the matter of the target and gives rise to a cascade whose excessive negative charge generates Cherenkov radio emission propagating within a cone of angular width $\Delta\theta_{\rm C}$. The radio wave crosses the surface, refracts according to the laws of geometrical optics, and propagates in space a large distance ($R_{\rm s}$). By reaching the antenna A on board the spacecraft at the altitude h, the radio emission can be registered by the detector.

The capabilities of existing and planned experiments on the detection of UHECRs and UHENs are determined by the energy dependence of the aperture, which is related to the target's characteristics. The registration apertures of cosmic rays and neutrinos with energies of $10^{18} - 10^{25}$ eV were calculated by the Monte Carlo method for different targets. The detectors were assumed to be at the altitude $h = 1000$ km.

The electric field of radio emission was calculated according to the parametrization [82, 83]

$$\tilde{E}_{\rm f}\ [\mu{\rm V\,m^{-1}\,MHz^{-1}}] = N\,\frac{ET_{\rm s}}{R_{\rm s}}\,\exp\left[-\alpha(E)(\cos\theta - \cos\theta_{\rm C})^2\right]\,\frac{\sin\theta}{\sin\theta_{\rm C}}\,.$$

In this formula, the following notation was introduced:

$$N = \frac{N_0}{\rho}\,\frac{f/f_0}{1 + (f/f_0)^{1.44}}\,,$$

$f_0 = 3.3$ GHz, $\cos\theta_{\rm C} = 1/n$ is the cosine of the Cherenkov angle, n is the refraction coefficient of the soil, $R_{\rm s}$ [km] is the distance from the refraction point on the surface to the antenna, θ is the polar angle of emission in the target's matter relative to the cascade direction, $T_{\rm s}$ is the transmission coefficient for the longitudinal polarization, E is the cascade energy [TeV], f is the frequency [GHz], ρ is the matter density, and $N_0 = 1.05 \times 10^{-4}$ μV m^{-1} MHz^{-1}. The $\alpha(E)$ function characterizes the angular width of radio emission and depends on the radiation length $L_{\rm rad}$ and the refraction coefficient n:

$$\alpha(E) \approx C^2 f^2 (A + B \ln E)\,,$$

where $A = 3413$, $B = 163$, and

$$C \approx \frac{L_{\rm rad}}{L_{\rm rad}^{\rm ice}}\,\frac{n}{n_{\rm ice}}\,.$$

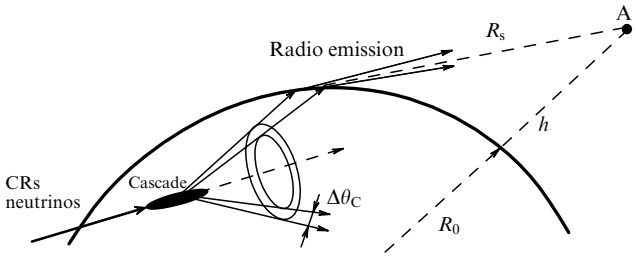

Figure 2. Schematic of the registration of cosmic rays and neutrinos by a radio antenna A on board a spacecraft.

The angular distribution of $\tilde{E}_f$ for different media in the energy range $10^{18} - 10^{25}$ eV is depicted in Fig. 3.

The radiation length $L_{\rm rad}$ in the regolith that was calculated using data on the chemical composition of the regolith, collected in space experiments Apollo-14, Apollo-16, Luna-16, and Luna-20 during flights to the Moon, was $L_{\rm rad}({\rm reg}) = 13.5$ cm, and for basalt $L_{\rm rad}({\rm basalt}) = 8$ cm.

The interaction length of cosmic rays is determined by the length $L_{\rm pN}$ of proton–nucleon (pN) interaction, and for neutrinos by the length $L_{\nu{\rm N}}$ of neutrino–nucleon (νN) interaction. At an energy of $\sim 10^8$ GeV, the cross section of the pN interaction is $\sigma_{\rm pN} \approx 10^{-25}$ cm^2, and for matter with

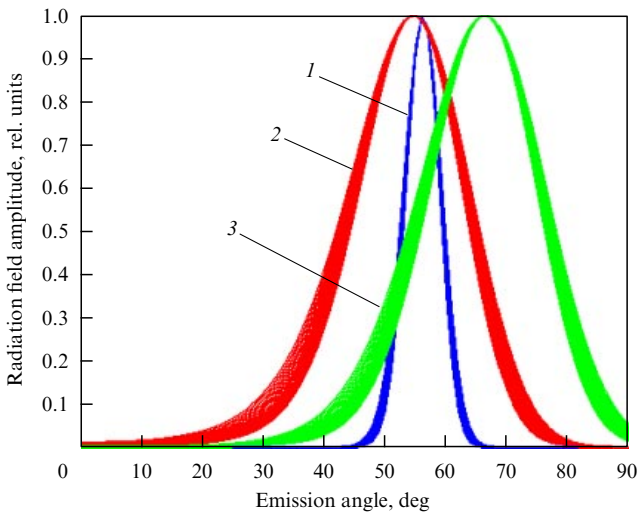

Figure 3. The angular distribution of Cherenkov radio emission at the frequency 200 MHz from cascades with particle energies of $10^{18} - 10^{25}$ eV for ice (*1*), the regolith (*2*), and basalt (*3*).

Table 1. The main characteristics of targets that are utilized in radio detection of UHECRs and UHENs.

Medium	ρ, g cm^{-3}	n	$L_{\rm rad}$, cm	$L_{\nu N}$ ($E_\nu = 10^{18}$ eV), km	$\lambda_{\rm abs}$ (f [GHz]), m
Ice	0.92	1.8	39	1250	$5000 \times f^{-0.3}$
Regolith	1.8	1.73	13.5	640	$18/f$
Basalt	3.0	2.5	8.0	380	$9/f$

density $\rho = 0.92-3.0$ g cm^{-3} the interaction length of cosmic rays is less than several centimeters. The ratio $\lambda_{\rm abs}/L_{\rm pN}$ is much larger than unity and hence all the cascades are initiated by cosmic rays so close to the surface that the absorption of emitted radio waves can be neglected (the 'surface target'). As the cross section $\sigma_{\nu N}$ of the νN interaction at energy $\sim 10^8$ GeV is almost five orders of magnitude smaller than $\sigma_{\rm pN}$, the length $L_{\nu N} \gg L_{\rm pN}$ reaches several hundred kilometers. For example, the neutrino interaction length in ice is $L_{\nu N}(10^{18}\ {\rm eV}) \approx 1250$ km. The cross section $\sigma_{\nu N}$ increases with energy, and in the energy range $10^{18}\ {\rm eV} \leqslant E_\nu \leqslant 10^{25}$ eV it can be approximated by the expression [84]

$$\sigma_{\nu N}(E_\nu) = 7.84 \times 10^{-36}\ {\rm cm}^2 \left(\frac{E_\nu}{1\ {\rm GeV}}\right)^{0.363}.$$

The probability of detecting radio emission from cascades is proportional to the ratio $\lambda_{\rm abs}/L_{\nu N}$, so the Moon and other space bodies constitutes volume targets for neutrinos.

The modeling algorithm was as follows. First, the number $N_{\rm CR}(E)$ or $N_\nu(E)$ of particles incident on the target's surface according to the energy spectra E^{-k} (k is the exponent of the spectrum slope for cosmic rays or neutrinos) was determined. Then, the spherical coordinates $(\theta_{\rm s}, \varphi_{\rm s})$ of the incident points of particles, the angles $(\theta_{\rm n}, \varphi_{\rm n})$ of incident directions of particles, the energy E, and, in the case of neutrinos, the interaction depth z were randomly chosen. At the next step, the strength $\tilde{E}_f$ of the radio emission field was calculated with account for the emission geometry, absorption in the radio-transparent medium, the transmission coefficient at the matter–vacuum boundary, and the attenuation due to increasing distance $R_{\rm s}$. The significant events were selected by simultaneous exceeding the threshold field $\tilde{E}_{\rm th} = 0.1\ \mu{\rm V\ m^{-1}\ MHz^{-1}}$ at three frequencies: 200, 300, and 400 MHz. The target characteristics listed in Table 1 were used in computations.

The total aperture $A(E)$ is calculated by integrating the angular aperture $\Delta\Omega(\theta_{\rm s}, \varphi_{\rm s}, E)$ over the visible target's surface:

$$A(E) = 2\pi R_0^2 \int_{\cos\theta_0}^{1} \Delta\Omega(\theta_{\rm s}, \varphi_{\rm s}, E)\, {\rm d}\cos\theta_{\rm s},$$

where R_0 is the target radius, h is the height of the orbit, $1 \geqslant \cos\theta_{\rm s} \geqslant \cos\theta_0$, and $\cos\theta_0 = R_0/(R_0 + h)$. For cosmic rays, only the upper hemisphere ($\cos\theta_{\rm n} > 0$) contributes to the angular aperture $\Delta\Omega_{\rm CR}$:

$$\Delta\Omega_{\rm CR} = \int \cos\theta_{\rm n}\, \Theta\left[\tilde{E}_f(E, \theta_{\rm s}, \theta) - \tilde{E}_{\rm th}\right] \Theta(\cos\theta_{\rm n})\, {\rm d}\varphi_{\rm n}\, {\rm d}\cos\theta_{\rm n},$$

where $\Theta(x)$ is the Heaviside step function: $\Theta = 0$ for $x < 0$, and $\Theta = 1$ for $x \geqslant 0$. Both upper and lower hemispheres are important for the neutrino contribution to the angular aperture $\Delta\Omega_\nu$. After integrating over the depth z, we obtain

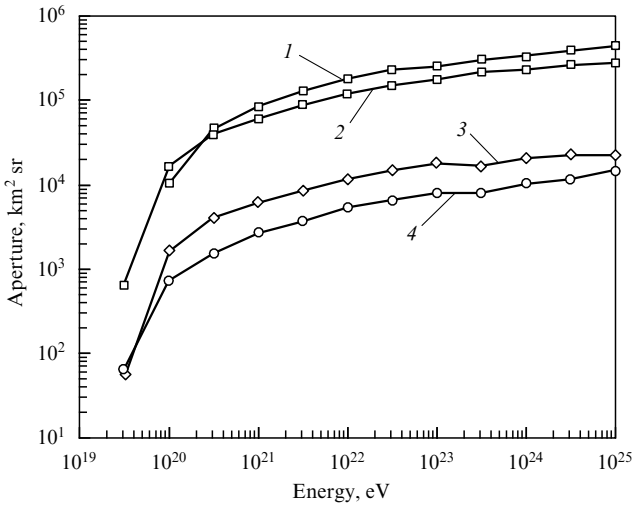

Figure 4. Apertures of different moon-targets for UHECR registration. Curves *1* and *2* correspond to targets with the regolith and basalt densities, respectively; curves *3* and *4* show apertures of the ice planets Ganymede and Europa, respectively.

the angular aperture for neutrinos:

$$\Delta\Omega_\nu = \int \frac{{\rm d}z}{L_{\nu N}} \int \Theta\left[\tilde{E}_f(E_\nu, \theta_{\rm s}, \theta) \exp\left(-\frac{z}{2\lambda_{\rm abs}}\right) - \tilde{E}_{\rm th}\right] \times \exp\left(-\frac{L(z, \theta_{\rm n})}{L_{\nu N}(E_\nu)}\right) {\rm d}\varphi_{\rm n}\, {\rm d}\cos\theta_{\rm n},$$

where the exponential factors describe the radio wave absorption under the surface of the target and the neutrino absorption in the target's matter in the path of length $L(z, \theta_{\rm n})$ to the point of cascade formation.

The results of modeling revealed a decrease in the apertures for cosmic rays and neutrinos with decreasing target radius. For example, the aperture of the largest ice moon in the Solar System, Ganymede ($R_0 = 2630$ km), is almost 40 times larger than that of the smallest ice moon, Enceladus ($R_0 = 252$ km). For comparison with the lunar target, the largest Jupiter satellites, Ganymede and Europa, were chosen. The lunar target was considered as a homogeneous solid body with the properties of either the regolith or basalt. The results of the aperture calculations are given in Figs 4 and 5 for UHECRs and UHENs, respectively. Figure 4 demonstrates that the aperture of the Moon for UHECR registration is an order of magnitude larger than that of ice moon-targets in the whole energy range considered. For UHEN registration, the situation is somewhat different (see Fig. 5). In the neutrino energy range $3 \times 10^{19} \leqslant E_\nu \leqslant 3 \times 10^{22}$ eV, apertures of moon-targets exceed those of the lunar target. However, the situation is similar to that for UHECRs for the highest neutrino energies ($E_\nu \approx 10^{24}-10^{25}$ eV) — the aperture of the

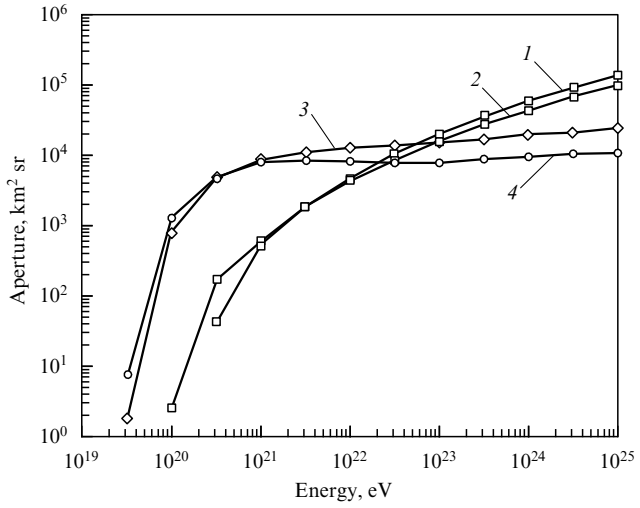

Figure 5. Apertures of different moon-targets for UHEN registration. Curves are labeled as in Fig. 4.

lunar target becomes significantly greater than that of ice moon-targets.

6. Conclusion

In the present paper, an analysis of possibilities of using Jupiter's and Saturn's ice satellites as targets for registration of UHECRs and UHENs by orbiting radio detectors is carried out. The results are compared with those for the lunar target. The Monte Carlo method was applied to calculate apertures of planned experiments with radio detectors on spacecrafts. The calculations were carried out in the energy range $10^{18} - 10^{25}$ eV with account for the target's physical properties, such as density, radiation length, radio waves absorption length, refraction coefficient, and radius. Modeling has been performed for UHECRs and UHENs separately, because of significant differences in the pN- and νN-interaction cross sections. For UHECRs, the typical cross section is about 100 mb, and the interaction length is no more than several centimeters. So, all targets for UHECRs can be considered as surface targets, and radio wave absorption can be neglected. As the νN cross section is 5–6 orders of magnitude smaller than the pN cross section, the characteristic interaction length $L_{\nu N}$ for UHENs can be as long as several hundred kilometers. Thus, neutrino interaction can occur at significant depths under the surface and absorption of radio waves in the volume target must be taken into account.

The results of calculations show that the aperture of the Moon (3×10^5 km^2 sr) for the detection of UHECRs with energies of $3 \times 10^{19} \leqslant E_{CR} \leqslant 10^{25}$ eV is an order of magnitude greater than that of the largest ice object in the Solar System, the Jovian satellite Ganymede (2×10^4 km^2 sr).

In the energy range $3 \times 10^{19} \leqslant E_\nu \leqslant 3 \times 10^{22}$ eV, the apertures of ice targets for UHENs exceed those of the lunar target. However, the aperture of the lunar target significantly increases at higher energies of neutrinos and reaches $\sim 10^5$ km^2 sr at $E_\nu = 10^{25}$ eV.

The characteristic features of UHECR and UHEN registration are due to the effect of the radio wave absorption length (λ_{abs}), the neutrino interaction length ($L_{\nu N}$), and the angular dependence of Cherenkov emission ($\Delta\theta_C$). It is shown that pure ice is, contrary to expectations, not an optimal material to detect UHECRs and UHENs. Despite the small attenuation of radio waves (λ_{abs} in ice comprises a few kilometers), the angular width of the Cherenkov radiation cone mostly affects the registration aperture which is 3–3.5 times smaller in ice than in the regolith or basalt.

The comparative analysis presented here showed that the Moon is more advantageous for radio detection of UHECRs and UHENs at the highest energies than the ice satellites of Jupiter and Saturn. Thus, within the Solar System there are no objects that can be utilized in space experiments for the detection of UHECRs and UHENs as an alternative to the future space mission Luna-Glob with the LORD orbital radio detector.

The work was done with partial support from RFBR grant 08-02-00515 and the RAS Program 'Neutrino Physics'.

References

1. Nagano M, Watson A A *Rev. Mod. Phys.* **72** 689 (2000)
2. Bertou X, Boratav M, Letessier-Selvon A *Int. J. Mod. Phys. A* **15** 2181 (2000); astro-ph/0001516
3. Halzen F, Hooper D *Rep. Prog. Phys.* **65** 1025 (2002); astro-ph/0204527
4. Torres D F, Anchordoqui L A *Rep. Prog. Phys.* **67** 1663 (2004); astro-ph/0402371
5. Anchordoqui L A, Montaruli T *Annu. Rev. Nucl. Part. Sci.* (submitted); arXiv:0912.1035
6. Ryabov V A *Usp. Fiz. Nauk* **176** 931 (2006) [*Phys. Usp.* **49** 905 (2006)]
7. Ryabov V A *Fiz. Elem. Chastits At. Yadra* **40** (1) 5 (2009) [*Phys. Part. Nucl.* **40** 1 (2009)]
8. Ryabov V A, Tsarev V A, Tskhovrebov A M *Usp. Fiz. Nauk* **178** 1129 (2008) [*Phys. Usp.* **51** 1091 (2008)]
9. Tsarev V A *Fiz. Elem. Chastits At. Yadra* **35** 187 (2004) [*Phys. Part. Nucl.* **35** 112 (2004)]
10. Grundy W M et al. *Science* **318** 234 (2007)
11. Gusev G A et al. *Kosmich. Issled.* **44** (1) 22 (2006) [*Cosmic Res.* **44** 19 (2006)]
12. Gusev G A et al. *Mat. Model.* **20** (6) 67 (2008)
13. Ryabov V A et al. *Nucl. Phys. B Proc. Suppl.* **196** 458 (2009)
14. Gusev G A et al. *Zh. Tekh. Fiz.* **80** (1) 98 (2010) [*Tech. Phys.* **55** 98 (2010)]
15. Ave M et al. *Phys. Rev. D* **65** 063007 (2002); astro-ph/0110613
16. Anchordoqui L, Goldberg H *Phys. Lett. B* **583** 213 (2004); hep-ph/0310054
17. Ivanov A A, Knurenko S P, Sleptsov I Ye *New J. Phys.* **11** 065008 (2009); arXiv:0902.1016
18. Takeda M et al. *Astropart. Phys.* **19** 447 (2003); astro-ph/0209422
19. Bird D J et al. *Astrophys. J.* **441** 144 (1995)
20. Abbasi R U et al. (High Resolution Fly's Eye Collab.) *Phys. Rev. Lett.* **100** 101101 (2008); astro-ph/0703099
21. Abraham J et al. (Pierre Auger Collab.) *Phys. Rev. Lett.* **101** 061101 (2008); arXiv: 0806.4302
22. Abraham J et al. (Pierre Auger Collab.) *Phys. Rev. D* **79** 102001 (2009); arXiv:0903.3385
23. Tameda Y (and the Telescope Array Experiment) *Nucl. Phys. B Proc. Suppl.* **196** 74 (2009)
24. Takahashi Y (and the JEM – EUSO Collab.) *New J. Phys.* **11** 065009 (2009); arXiv:0910.4187
25. Tkatchev L et al., in *Proc. of the 30th Intern. Cosmic Ray Conf., Merida, Mexico, 3–11 July 2007* Vol. 5 (Eds R Caballero et al.) (Mexico: Univ. Nac. Autonova de México, 2008)
26. Waxman E *Phys. Rev. Lett.* **75** 386 (1995); astro-ph/9505082
27. Vietri M *Astrophys. J.* **453** 883 (1995); astro-ph/9506081
28. Vietri M, De Marco D, Guetta D *Astrophys. J.* **592** 378 (2003); astro-ph/0302144
29. Piran T *Rev. Mod. Phys.* **76** 1143 (2004); astro-ph/0405503
30. Berezinskii V S et al. *Astrofizika Kosmicheskikh Luchei* (Astrophysics of Cosmic Rays) (Ed. V L Ginzburg) (Moscow: Nauka, 1984) [Translated into English (Amsterdam: North-Holland, 1990)]

31. Biermann P L, Strittmatter P A *Astrophys. J.* **322** 643 (1987)
32. Rachen J P, Biermann P L *Astron. Asrophys.* **272** 161 (1993); astro-ph/9301010
33. Rachen J P, Mészáros P *Phys. Rev. D* **58** 123005 (1998); astro-ph/9802280
34. Razzaque S, Mészáros P, Waxman E *Phys. Rev. Lett.* **90** 241103 (2003); astro-ph/0212536
35. Semikoz D, Sigl G *JCAP* **0404** 003 (2004); hep-ph/0309328
36. Bhattacharjee P, Hill C T, Schramm D N *Phys. Rev. Lett.* **69** 567 (1992)
37. Sigl G et al. *Phys. Rev. D* **59** 043504 (1999); hep-ph/9809242
38. Berezinsky V, Kachelriess M *Phys. Rev.* **63** 034007 (2001); hep-ph/0009053
39. Barbot C et al. *Phys. Lett. B* **555** 22 (2003); hep-ph/0205230
40. Aloisio R, Berezinsky V, Kachelriess M *Phys. Rev. D* **69** 094023 (2004); hep-ph/0307279
41. Berezinsky V S, Zatsepin G T *Phys. Lett. B* **28** 423 (1969)
42. Yoshida S, Teshima M *Prog. Theor. Phys.* **89** 833 (1993)
43. Yoshida S et al. *Astrophys. J.* **479** 547 (1997); astro-ph/9608186
44. Kalashev O E et al. *Phys. Rev. D* **66** 063004 (2002); hep-ph/0205050
45. Engel R, Seckel D, Stanev T *Phys. Rev. D* **64** 093010 (2001); astro-ph/0101216
46. Allard D et al. *JCAP* **0609** 005 (2006); astro-ph/0605327
47. Anchordoqui L A et al. *Phys. Rev. D* **76** 123008 (2007); arXiv:0709.0734
48. DeYoung T (and IceCube Collab.) *Proc. of the DPF-2009 Conf., Detroit, MI, July 27–31, 2009*; arXiv:0910.3644
49. Aynutdinov V et al. (and the BAIKAL Collab.) *Astropart. Phys.* **25** 140 (2006); astro-ph/0508675
50. Ackermann M et al. *Astrophys. J.* **675** 1014 (2008); arXiv:0711.3022
51. Kravchenko I et al. *Phys. Rev. D* **73** 082002 (2006); astro-ph/0601148
52. Abbasi R U et al. *Astrophys. J.* (submitted); arXiv:0803.0554
53. Gorham P et al. (ANITA Collab.) *Phys. Rev. Lett.* **103** 051103 (2009); arXiv:0812.2715
54. Gorham P et al. *Phys. Rev. D* (submitted); arXiv:1003.2961
55. Gorham P W et al. *Phys. Rev. Lett.* **93** 041101 (2004); astro-ph/0310232
56. Lehtinen N G et al. *Phys. Rev. D* **69** 013008 (2004); astro-ph/0309656
57. Scholten O et al. *Nucl. Instrum. Meth. Phys. Res. A* **604** (Suppl. 1) S102 (2009); *Contribution to the Arena 2008 Conf., Rome, 25–27 June 2008*; arXiv:0810.3426
58. Scholten O et al. *Phys. Rev. Lett.* **103** 191301 (2009); arXiv:0910.4745
59. Horneffer A et al. *Nucl. Instrum. Meth. Phys. Res. A* **604** (Suppl. 1) S20 (2009); arXiv:0903.2398
60. Chirkin D for Ice Cube Collab., in *Contribution to 31st ICRC, Lódź, 2009*, HE 2.2 1418
61. Gaisser T K, Honda M *Annu. Rev. Nucl. Part. Sci.* **52** 153 (2002); hep-ph/0203272
62. Volkova L V, Zatsepin G T *Yad. Fiz.* **64** 313 (2001) [*Phys. At. Nucl.* **64** 266 (2001)]
63. Barr G D et al. *Phys. Rev. D* **70** 023006 (2004); astro-ph/0403630
64. Beacom J F, Candia J *JCAP* **0411** 009 (2004); hep-ph/0409046
65. Honda M et al. *Phys. Rev. D* **75** 043006 (2007); astro-ph/0611418
66. Enberg R, Reno M H, Sarcevic I *Phys. Rev. D* **78** 043005 (2008); arXiv:0806.0418
67. Cronin J, Gaisser T, Swordy S *Sci. Am.* **276** (1) 44 (1997)
68. Aguilar J A et al. *Astropart. Phys.* **26** 314 (2006); astro-ph/0606229
69. Aggouras G et al. (NESTOR Collab.) *Astropart. Phys.* **23** 377 (2005)
70. Aiello S et al. *Astropart. Phys.* **33** 263 (2010); arXiv:0910.1269
71. Rapidis P A (and the KM3NeT Consortium) *J. Phys. Conf. Ser.* **120** 062011 (2008); arXiv:0803.2478
72. Abbasi R et al. (IceCube Collab.) *Phys. Rev. Lett.* **103** 221102 (2009); arXiv:0911.2338
73. Barwick S W *J. Phys. Conf. Ser.* **60** 276 (2007); astro-ph/0610631
74. Gorham P et al. *Nucl. Instrum. Meth. Phys. Res. A* **490** 476 (2002); hep-ex/0108027
75. James C W et al. *Mon. Not. R. Astron. Soc.* **379** 1037 (2007); astro-ph/0702619
76. Falcke H, Gorham P, Protheroe R J *New Astron. Rev.* **48** 1487 (2004); astro-ph/0409229
77. James C W, Protheroe R J *Astropart. Phys.* **30** 318 (2009); arXiv:0802.3562
78. James C W et al. *Phys. Rev. D* **81** 042003 (2010); arXiv:0911.3009
79. Askar'yan G A *Zh. Eksp. Teor. Fiz.* **41** 616 (1961) [*Sov. Phys. JETP* **14** 441 (1962)]
80. Askar'yan G A *Zh. Eksp. Teor. Fiz.* **48** 988 (1965) [*Sov. Phys. JETP* **21** 658 (1965)]
81. Dagkesamanskii R D, Zheleznykh I M *Pis'ma Zh. Eksp. Teor. Fiz.* **50** 233 (1989) [*JETP Lett.* **50** 259 (1989)]
82. Zas E, Halzen F, Stanev T *Phys. Rev. D* **45** 362 (1992)
83. Alvarez-Muñiz J et al. *Phys. Rev. D* **74** 023007 (2006); astro-ph/0512337
84. Gandhi R et al. *Phys. Rev. D* **58** 093009 (1998); hep-ph/9807264